Available online at www.sciencedirect.com
ScienceDirect
Nuclear Instruments and Methods in Physics Research A 581 (2007) 84–87
NUCLEAR INSTRUMENTS & METHODS IN PHYSICS RESEARCH Section A
www.elsevier.com/locate/nima

A single photon emission computer tomograph for breast cancer imaging

S. Vecchio[a,*], N. Belcari[a], P. Bennati[b], M. Camarda[a], R. Campanini[c], M.N. Cinti[b], A. Del Guerra[a], E. Iampieri[c], N. Lanconelli[c], R. Pani[b], L. Spontoni[a]

[a]Department of Physics "E. Fermi", University of Pisa and INFN-Pisa, Largo B. Pontecorvo 3, I-56127 Pisa, Italy
[b]University "La Sapienza" and INFN-Roma I, Rome, Italy
[c]University of Bologna and INFN-Bologna, Bologna, Italy

Available online 24 July 2007

Abstract

We have developed a tomograph for single photon emission imaging (SPECT) of the breast for the detection of small size tumors. The SPECT is mounted on a ring that is rotating around the breast with the patient in prone position. The breast will be imaged by two opposing detector heads of approximately $5 \times 15\,cm^2$ each, with a field of view about 13 cm wide. Each head is made up of one pixilated NaI crystal matrix coupled to three Hamamatsu H8500 PMTs. A "general purpose" lead collimator is positioned in front of the crystal. Detailed simulations have been made for the optimization and the evaluation of the detector performances. Monte Carlo results indicate that tumors of 8 mm diameter are detectable with a tumor/background uptake ratio of 5:1. The experimental characterization of the detector head is presented. The rotating ring is now being assembled.

PACS: 01.30.Cc; 07.85.−m; 29.40.Mc; 27.57.uh

Keywords: SPECT; MA-PMT; Breast cancer

1. Introduction

We have developed a tomograph for single photon emission computed tomography (SPECT) imaging of the breast that could overcome the present clinical sensitivity limit (about 1 cm tumor diameter) for the detection of small size tumors. The long term objective is to be able to perform the analysis of ^{99m}Tc radiopharmaceutical perfusion uptake rate due to neoangiogenesys generated from the presence of the lesion [1]. On the other hand, a standard 20 min scan after the uptake will give the classic tomographic image of the cellular steady-state model, to confirm the presence of higher radioactivity uptake from malignant lesions.

The patient is in prone position, with a pendulus breast. The SPECT system is mounted on a ring that is rotating around the breast.

2. The tomographic system

2.1. Mechanical assembly

The compact SPECT ring adapts to the breast anatomy in order to achieve high-spatial resolution. The detection system (Fig. 1) is made of two small gamma cameras, each $5 \times 15\,cm^2$ in dimension.

Each head has three 64-anodes PMT Hamamatsu H8500 [2]. The H8500 PMT has an external size of $52.0 \times 52.0\,mm^2 \times 12.7\,mm$. The photocathode is bialkali and the glass window is 1.5 mm thick. The nominal active area of each PSPMT is $49 \times 49\,mm^2$. The dead zone is about 1.5 mm for each side, thus allowing a close packing. However, because of subsampling limits of the peripheral

*Corresponding author. Tel.: +39 50 2214940; fax: +39 50 2214333.
E-mail address: sara.vecchio@pi.infn.it (S. Vecchio).

0168-9002/$ - see front matter
doi:10.1016/j.nima.2007.07.034

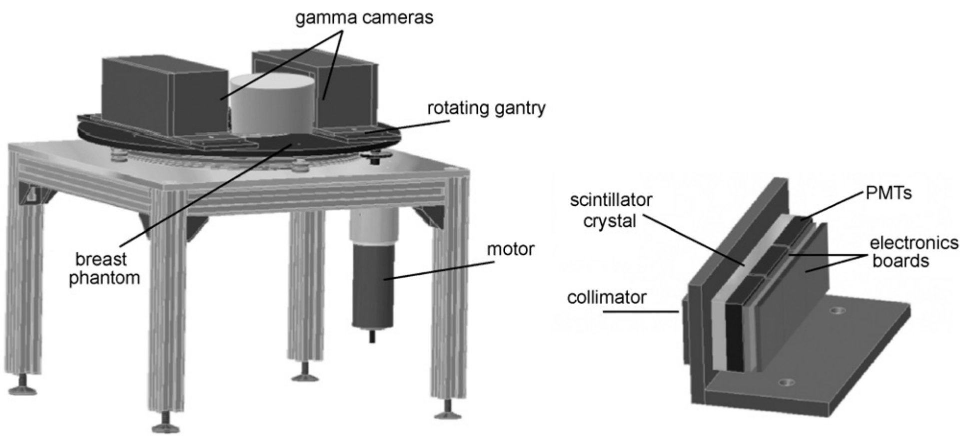

Fig. 1. Left: the mechanical assembly of the rotating SPECT ring. Right: conceptual design of a single head.

anode pads, the effective useful active area is $46 \times 46\,\mathrm{mm}^2$ only, if the event localization as derived from each PMT is used separately.

The PMT triplet is coupled to a $5 \times 15\,\mathrm{cm}^2$ matrix of NaI(Tl), 2.2 mm pitch and 6 mm thickness, with a glass entrance window of 3 mm. The readout system developed for the 3-PMT assembly enables the recovering of the events falling in the dead area between the tubes (see Section 2.3).

The total amount of glass placed between the crystal and the photocathode (4.5 mm) introduces a wide light spread for each single event. Such a broad distribution makes the light spot to be sampled by at least three anode pads. Since the effective dead area is about 8 mm, even those events falling between two PMTs can be recovered if information derived by both tubes is combined.

The total detecting area is then $46 \times 150\,\mathrm{cm}^2$. "General purpose" collimators have been chosen, 22 mm thick, with 1.5 mm holes and 0.2 mm septa, after an accurate Monte Carlo simulation of several possibilities [3].

The radius of rotation is 6.5 cm, thus allowing SPECT investigation up to a 13 cm diameter breast. Compactness allows a drastic weight reduction of the gamma camera (about 10 kg).

2.2. Simulation

The tomographic reconstruction is performed through an iterative algorithm based on simulated annealing technique. The real projections are perturbed and accepted for the following iteration if they minimize the cost function:

$$E = S \cdot \sum_{j=1}^{N_\mathrm{p}} |A_j - \langle A \rangle_n| + (1 - S)\frac{\sum_{k,m}(P_{k,m} - P_{k,m}^{\mathrm{rec}})^2}{K \cdot M} \qquad (1)$$

where N_p is the number of image pixels, $\langle A \rangle_n$ is the average activity in a region $n \times n$ around the pixel of interest, S is the smoothing parameter, $P_{k,m}$ and $P_{k,m}^{\mathrm{rec}}$ are the measured projections and pseudo-projection, respectively, for the kth detection element at angle m.

Each detector head acquires 18 projections over 180°. The energy E_γ of the photons from $^{99\mathrm{m}}$Tc is 140 keV, and reconstructed events are those above the energy threshold $E_\gamma - 2\sigma_\mathrm{E}$. The reconstruction considers the collimator response, which introduces different light spread at the various distances. Corrections for breast tissue attenuation and variable spatial resolution of the camera are also applied when calculating the pseudo-projections at each iteration of the reconstruction procedure. Scattering corrections which have a minor influence on the reconstruction of homogeneous phantoms therefore have not been implemented.

A complete simulation of the SPECT ring [3] with the EGSnrc code has been performed. The simulation of the detector shows that the system has the capability to detect tumors of 8 mm diameter with a tumor/background uptake ratio of 5:1 (see Fig. 2). The figures of merit used for the analysis of MC simulation are signal-to-noise ratio (SNR) and image contrast (IC), defined as follows:

$$\mathrm{SNR} = \frac{\Sigma_{\mathrm{ROI}} - \mathrm{BKG}}{\sigma_{\mathrm{BKG}}} \qquad (2)$$

$$\mathrm{IC} = \frac{\Sigma_{\mathrm{ROI}} - \mathrm{BKG}}{\Sigma_{\mathrm{BKG}}} \qquad (3)$$

where BKG is the background average, σ_{BKG} is the background standard deviation, and Σ_{ROI} is the average over a ROI centered on the tumor.

2.3. Readout electronics

A multiplexed setup based on Symmetric Charge Division (SCD, [4]) resistive networks has been chosen for the readout of each individual PMT as the best compromise between performances and simplicity. The SCD resistive network reduces the 8×8 signals of each PMT to $8 + 8$ signals. The eight signals enter a passive resistive chain that further reduces the number of signals to 2. The digitization and acquisition of the $2 + 2$ signals of each head is then made through a dedicated electronics board (see Fig. 3). The last dynode output signals from the

PMTs are amplified by fast, low-noise pre-amplifiers. A constant fraction discriminator (CFD) for each photomultiplier tube is then used for amplitude-independent gate generation for the acquisition of the position signals. When one last-dynode signal passes the CFD, the $2 \times (2+2)$ position signals from that tube and its neighbor(s) are digitized by a system composed by a peak detector plus a peak sensing ADC. The digital data are then transferred to a local PC server via USB2 connection.

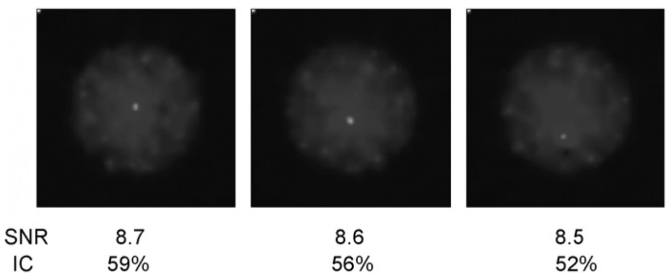

Fig. 2. Example of a reconstructed slice for an 8 mm diameter spherical tumor (T/B 5 : 1) within a 10 cm diameter cylindrical breast phantom. Left: tumor on the rotation axis. Center: tumor shifted 1 cm from the rotation axis. Right: tumor shifted 2 cm from the rotation axis.

Each PMT is separately readout, but time correlation is available to individualize the events shared by two PMTs, i.e., those happening in the dead area between the detector elements. The large light yield from NaI crystal makes such partial information still detectable, since the signal from at least one of the two PMTs involved by a dead-area event passes the trigger threshold (set up at about 40 keV). The three PMT planar images for each head are then combined by software before the sinogram construction.

3. Results and future work

Previous results for ^{22}Na on YAP pixilated crystals coupled to a single H8500 PMT with SCD-based multiplexed readout showed an intrinsic spatial resolution below 1.5 mm (FWHM) [5]. The energy resolution for ^{57}Co on a NaI(Tl) crystal (1.8 mm pixel) coupled to a single H8500 PMT was found to be about 16% and the peak to valley ratio finally was higher than 6 [6].

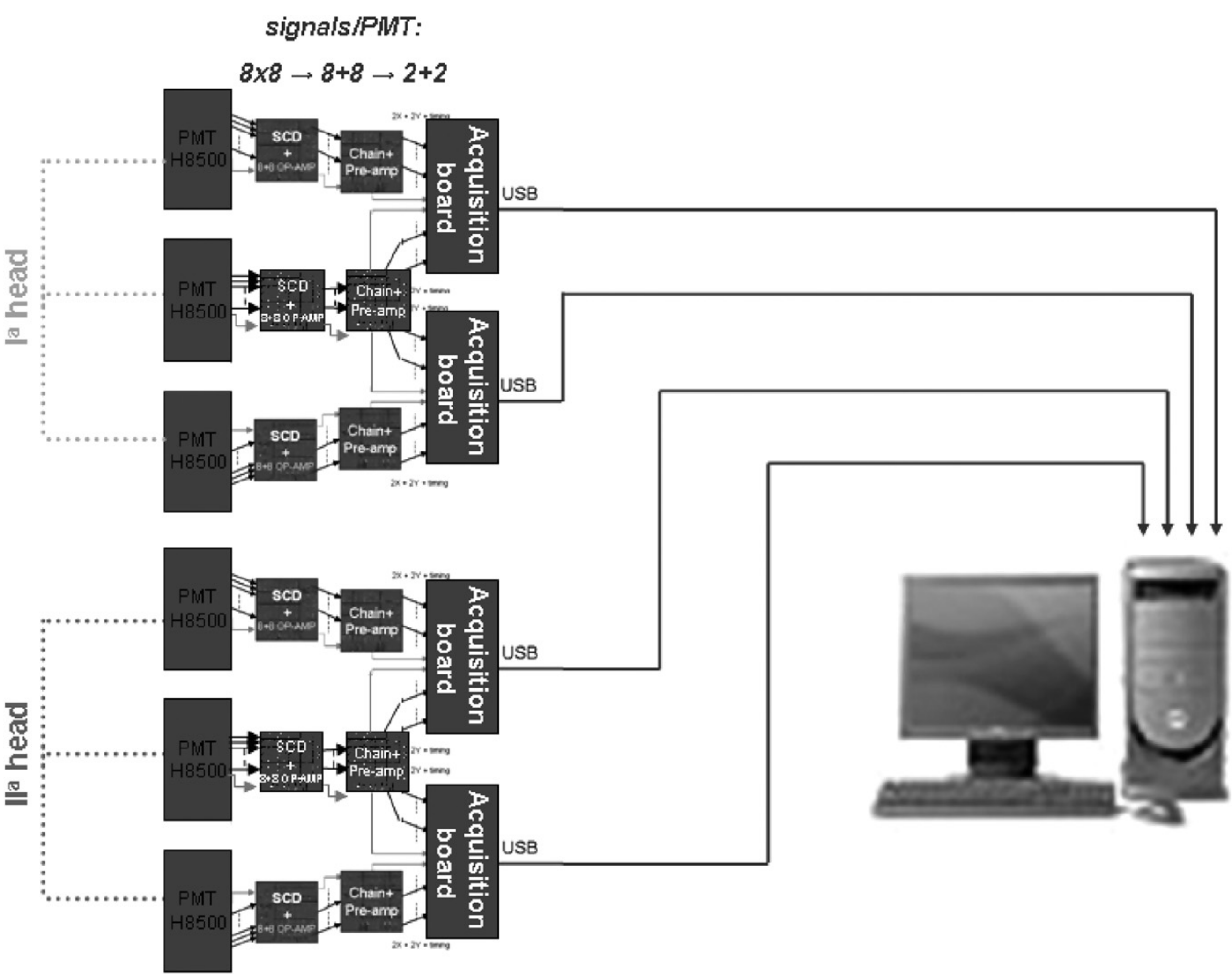

Fig. 3. Readout architecture for the entire tomograph.

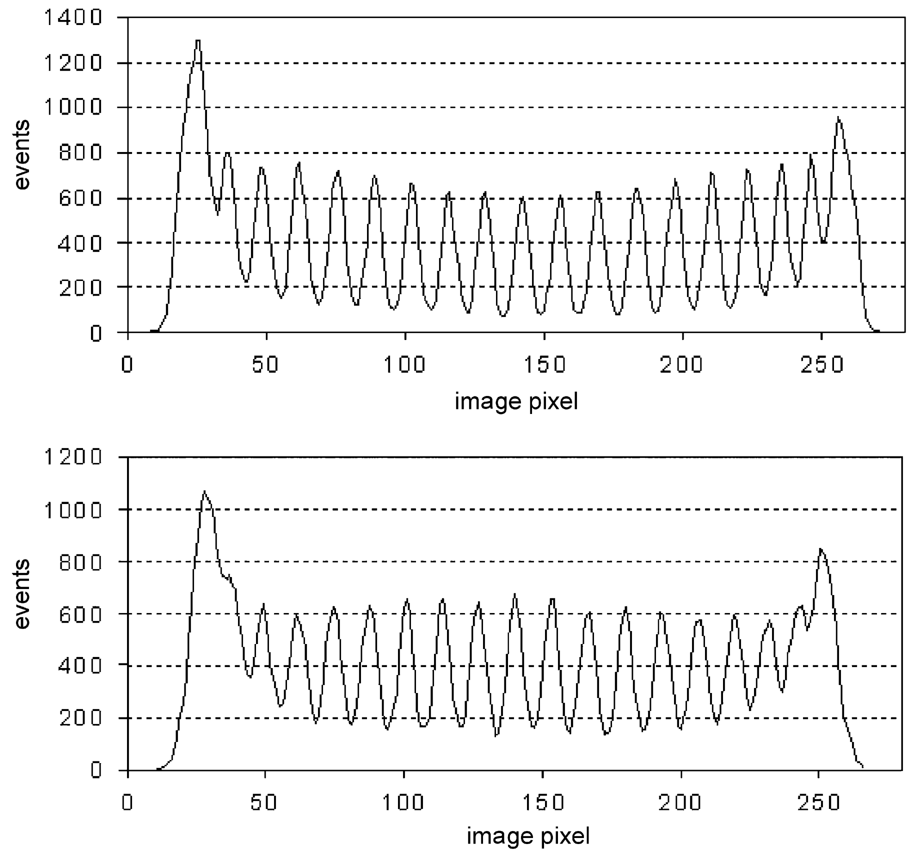

Fig. 4. Vertical profiles for a ^{57}Co flood field image of one head (without collimator). Top: profile extracted from an active area. Bottom: profile extracted from a dead area.

For the triplet assembly presented in this article—i.e., three H8500 PMT coupled to a single large NaI(Tl) crystal (2 mm pixel)—the peak to valley ratio in the vertical direction is 4.6 and 3.2 for the active area and the dead area, respectively (see Fig. 4). The result along the horizontal direction is slightly worse, reaching an average of 2.5 for a total row of 67 crystal pixels. The spatial resolution is always below 1.3 mm (FWHM). The energy resolution for ^{57}Co irradiation of NaI is about 16% in the active area and 18% in the recovered dead area.

The realization of the two heads has been recently completed, and the rotating ring has been constructed. The SPECT ring will be transferred to the Nuclear Medicine Division of the University of Pisa, to perform the validation on breast phantoms.

Acknowledgment

The research was partially supported by the MIUR, in the framework of the PRIN2004 program, number 2004028450, “New Techniques for Breast Cancer Imaging”.

References

[1] N. Weidner, et al., J. Natl. Cancer Inst. 84 (1992) 1875.
[2] Hamamatsu Technical Information, H8500 PSPMT, Japan, 2003.
[3] N. Lanconelli, et al., Conference Records of 2006 IEEE NSS/MIC/RTSD, San Diego, USA, M14-18.
[4] P.D. Olcott, et al., IEEE Trans. Nucl. Sci. NS-52 (2005) 21.
[5] S. Vecchio, et al., Nucl. Instr. and Meth. A 569 (2006) 264.
[6] N. Belcari, et al., Nucl. Instr. and Meth. A 572 (2007) 335.